Development of an Advanced Mapped Real Transform for Enhanced Feature Extraction in Language Translation Application using Machine Learning

Lakshmi. S. Panicker, Rahul .C, R. Gopikakumari
School of Engineering, CUSAT

Abstract*— The majority of applications for signal processing involve changing signals from one domain to another. A common frequency domain representation is the discrete Fourier transform (DFT), which depicts the relative contribution of each frequency component in terms of complex sinusoids. The 2-D Mapped Real Transform (2-D MRT) is a very redundant and expansive transform that was proposed by changing 2-D DFT computations in terms of real additions by taking advantage of the periodicity and symmetry properties of the twiddle factor. Therefore, 2-D Unique MRT (2-D UMRT), which has the same size as the original signal, was proposed by detecting unique MRT coefficients. The phase components of a given frequency, however, are arranged in a scattered manner. The shortcomings of 2-D UMRT were addressed by the development of 2-D Sequency-based MRT (2-D SMRT). Still, only signals of size N with a power of 2 can be used with SMRT. MRT is extended for 1-D signals as well, while being developed initially for 2-D signals. The development of a new independent integer-to-integer transform, called 1-D GMRT, derived from 1-D MRT, is presented. It features the use of unique MRT coefficients that are ordered in terms of Greatest Common Divisor (GCD) values rather than sequency values for any N condition. The utilization of this transform in a speech translation application is also presented and in comparison, with traditional methods, the current system indicates an improvement of 10% in performance.

Index Terms*— DFT, GMRT, 1-D transform, Unique MRT, speech translation, language processing

I. INTRODUCTION

Transforms are tools that offer an alternate domain of representation for signal analysis. Discrete Fourier Transform (DFT) is the most widely used transform for frequency domain analysis of 1-D discrete-time signals. However, the main drawback of DFT is that all computations are carried out in complex domain resulting in increased computational complexity. Fast Fourier Transform (FFT) aimed to reduce the computational complexity of DFT. However, 2-D FFT resulted in reduced speed of processing since real data is also changed and processed in the complex domain.

A new approach was suggested in [1] to derive a modified DFT relation that performed all major computations in terms of real additions by expressing NxN DFT in terms of 2x2 DFT and utilizing the periodicity and symmetry properties of the twiddle factor. Further, the visual representation of 2-D DFT in terms of 2x2 DFT was explored and developed a four-layered parallel distributed architecture with real additions alone except for a scaling operation by twiddle factor in the final layer for $((N))_4 = 2$. It can give a representation of the signal in the complex domain in terms of real arithmetic if the fourth layer is eliminated. Hence, an independent transform called the Mapped Real Transform (MRT) was developed from the modified DFT relation based on number theory. It is an integer-to-integer transform as its kernel has only 1, -1, and 0 as elements. While DFT computations are performed in the complex domain, MRT represents complex domain information in terms of real additions. It represents a signal in terms of signal components that are mapped onto the twiddle factor axes and grouped according to the phase of the twiddle factor in terms of real arithmetic [2][3][4]. Moreover, each DFT coefficient can be derived from the MRT representation by multiplying each MRT coefficient with the corresponding twiddle factor and adding them together, involving only N/2 complex multiplications.

However, MRT is a highly redundant and expansive transform with $N^3/2$ coefficients rather than N^2 coefficients as it maps a 2-D signal of size $N \times N$ into M matrices each of size $N \times N$ where N is an even integer and $M = \frac{N}{2}$. So 2-D Unique MRT (2-D UMRT) was suggested for any even N to eliminate redundant coefficients by arranging the N^2 unique coefficients in an $N \times N$ matrix form and implementing them as a three-layer parallel distributed architecture in [4]. This

type of arrangement resulted in the scattered placement of phase components corresponding to a given frequency and posed issues in many applications. Hence, the visual representation of unique MRT coefficients was explored and 2-D Sequency based MRT (2-D SMRT) [5], [6] was derived by the arrangement of unique coefficients in accordance with their row and column sequencies. However, the application of SMRT is limited to cases where N is a power of 2. Although MRT, UMRT and SMRT were originally developed for 2-D signal processing applications, 1-D MRT was also developed in [2].

The unique MRT coefficients retained after the removal of redundancies in 1-D MRT are arranged into Greatest Common Divisor (GCD) packets called 1-D GCD based unique MRT (1-D GMRT) in [7]. It is applicable for 1-D signals of any even length N. Futher an improved representation of 1-D GMRT is suggested in this paper so as to develop it into a full-fledged integer transform. A detailed description algorithms developed to establish the new forward & inverse 1-D GMRT representation, its properties and a relevant application are presented.

II. 1-D MRT

Let Y_k, $0 \le k \le N-1$ be the DFT of a sequence $x(n)$, $0 \le n \le N-1$, then

$$Y_k = \sum_{n=0}^{N-1} x(n) W_N^{nk} \quad (1)$$

Direct computation of DFT is inefficient as it requires N^2 complex multiplications and $N(N-1)$ complex additions and was reduced with the use of divide and conquer approach based Fast Fourier Transform (FFT) algorithm [8] performed in the complex domain. Hence, total number of complex multiplications and additions involved are $\frac{N}{2}\log_2 N$ and $N \log_2 N$ respectively for N a power of 2 case.

A significant reduction of complex arithmetic involved in computation of DFT coefficients was achieved by exploiting symmetry and periodicity properties of twiddle factor, W_N^{nk}. Equation (1) was re-written using the periodicity property of twiddle factor, W_N^{nk}, as

$$Y_k = \sum_{n=0}^{N-1} x(n) W_N^{((nk))_N} \quad (2)$$

Equation (2) was modified by grouping the data at locations n that share the same value for the exponent $((nk))_N = p$ for a given value of frequency k and using symmetry property of twiddle factor as

$$Y_k = \sum_{p=0}^{M-1} Y_k^p W_N^p \quad (3)$$

$$Y_k^p = \sum_{\forall n|((nk))_N=p} x(n) - \sum_{\forall n|((nk))_N=p+M} x(n) \quad (4)$$

where $0 \le k \le N-1$, $0 \le p \le M-1$ and Y_k^p represents 1-D MRT of $x(n)$, k & p are frequency & phase indices respectively. Thus 1-D MRT [2] maps an array of length N into M arrays of length N each using real additions alone. Equation (3) gives the relation between 1-D DFT & 1-D MRT where MRT has two independent parameters, k & p, unlike DFT, ie., MRT maps a 1-D array into 2-D array.

Basis vectors of MRT coefficients for $N = 4$ are shown in Fig.1. The value of frequency index k provides information about number of frequency cycles present in the basis vectors.

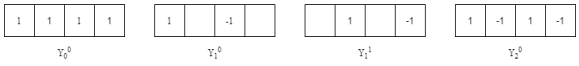

Fig. 1. Basis vectors of MRT coefficients for $N = 4$

For example, the MRT coefficient Y_1^0 of frequency $k = 1$ has the basis vector with one frequency cycle given by 1 and -1. Starting location of frequency cycle depends on the value of phase index p and phase shift in frequency domain corresponds to time shift in the time domain. Thus, phase index provides time information of the signal. Hence, MRT is a time-frequency representation. Detailed discussion on validity and number of phase indices p to be considered was presented in [7]. A few properties of 1-D MRT are discussed below.

A. Properties

1) General Properties

a) Linearity

If $x_1(n) \overset{MRT}{\longleftrightarrow} Y_{1_k}^p$ and $x_2(n) \overset{MRT}{\longleftrightarrow} Y_{2_k}^p$ then, $a_1x_1(n) + a_2x_2(n) \overset{MRT}{\longleftrightarrow} a_1Y_{1_k}^p + a_2Y_{2_k}^p$ for any real valued constants a_1 & a_2

Proof

From (4), $\sum_{\forall n|((nk))_N=p} x(n) - \sum_{\forall n|((nk))_N=p+M} x(n) = Y_k^p$ then

$$\sum_{\forall n|((nk))_N=p}\big(a_1x_1(n) + a_2x_2(n)\big) - \sum_{\forall n|((nk))_N=p+M}\big(a_1x_1(n) + a_2x_2(n)\big)$$
$$= a_1\Big(\sum_{\forall n|((nk))_N=p} x_1(n) - \sum_{\forall n|((nk))_N=p+M} x_1(n)\Big) + a_2\Big(\sum_{\forall n|((nk))_N=p} x_2(n) - \sum_{\forall n|((nk))_N=p+M} x_2(n)\Big)$$
$$= a_1\big(Y_{1_k}^p\big) + a_2\big(Y_{2_k}^p\big)$$

b) Signal reversal

If $x(n) \overset{MRT}{\longleftrightarrow} Y_k^p$ and $x((-n))_N \overset{MRT}{\longleftrightarrow} Y'^p_k$,

then $Y'^{p}_{k} = sY_k^{((M-p))_M}$, $s = \begin{cases} 1, & p = 0 \\ -1, & p \neq 0 \end{cases}$

Proof

$x((-n))_N \xleftrightarrow{MRT} Y'^{p}_{k}$

$Y'^{p}_{k} = \sum_{\forall n|((nk))_N=p} x((-n))_N - \sum_{\forall n|((nk))_N=p+M} x((-n))_N$

Let $((-n))_N = ((N-n))_N = n'$

$Y'^{p}_{k} = \sum_{\forall n'|((((-n'))_N k))_N=p} x(n') - \sum_{\forall n'|((((-n'))_N k))_N=p+M} x(n')$

$Y'^{p}_{k} = \sum_{\forall n'|((n'k))_N=((N-p))_N} x(n') - \sum_{\forall n'|((n'k))_N=((N-(p+M)))_N} x(n')$

$Y'^{p}_{k} = \sum_{\forall n'|((n'k))_N=((M-p+M))_N} x(n') - \sum_{\forall n'|((n'k))_N=((M-p))_N} x(n')$

$$Y'^{p}_{k} = -Y_k^{M-p} = sY_k^{((M-p))_M}, s = \begin{cases} 1, & p = 0 \\ -1, & p \neq 0 \end{cases}$$

c) Circular shift

If $x(n) \xleftrightarrow{MRT} Y_k^p$ & $x'(n) = x((n-l))_N \xleftrightarrow{MRT} Y'^{p}_{k}$,

then $Y'^{p}_{k} = sY_k^{((p-lk))_M}$, $s = \begin{cases} 1, ((p-lk))_N < M \\ -1, ((p-lk))_N \geq M \end{cases}$

Proof

$Y'^{p}_{k} = \sum_{\forall n|((nk))_N=p} x'(n) - \sum_{\forall n|((nk))_N=p+M} x'(n)$

$Y'^{p}_{k} = \sum_{\forall n|((nk))_N=p} x((n-l))_N - \sum_{\forall n|((nk))_N=p+M} x((n-l))_N$

Substituting $n' = ((n-l))_N$

$Y'^{p}_{k} = \sum_{\forall n'|((n'k))_N=((p-lk))_N} x(n') - \sum_{\forall n'|((n'k))_N=((p-lk+M))_N} x(n')$

$$Y'^{p}_{k} = -Y_k^{((p-lk))_M} = sY_k^{((p-lk))_M}, s = \begin{cases} 1, & ((p-lk))_N < M \\ -1, & ((p-lk))_N \geq M \end{cases}$$

When a signal $x(n)$ is circularly shifted as $x'(n) = x((n-l))_N$, each MRT coefficient undergoes a shift in p along with possible sign change.

d) Circular Convolution

If $x_1(n) \xleftrightarrow{MRT} Y_{1_k}^p$ & $x_2(n) \xleftrightarrow{MRT} Y_{2_k}^p$ and

$x'(n) = \sum_{j=0}^{N-1} x_1(j)x_2((n-j))_N \xleftrightarrow{MRT} Y'^{p}_{k}$

then $Y'^{p}_{k} = \sum_{j=0}^{M-1} sY_{1_k}^{((jk))_N} Y_{2_k}^{\left((p-((jk))_N)\right)_M}$,

$$s = \begin{cases} 1, ((jk))_N < p+1 \\ -1, ((jk))_N \geq p+1 \end{cases}$$

Proof

$x'(n) = \sum_{j=0}^{N-1} x_1(j)x_2((n-j))_N$

$Y'^{p}_{k} = \sum_{\forall n|((nk))_N=p} x'(n) - \sum_{\forall n|((nk))_N=p+M} x'(n)$

$Y'^{p}_{k} = \sum_{\forall n|((nk))_N=p} \sum_{j=0}^{N-1} x_1(j)x_2((n-j))_N - \sum_{\forall n|((nk))_N=p+M} \sum_{j=0}^{N-1} x_1(j)x_2((n-j))_N$

$Y'^{p}_{k} = \sum_{j=0}^{N-1} \left[\sum_{\forall n|((nk))_N=p} x_1(j)x_2((n-j))_N - \sum_{\forall n|((nk))_N=p+M} x_1(j)x_2((n-j))_N\right]$

$Y'^{p}_{k} = \sum_{j=0}^{N-1} x_1(j) \left[\sum_{\forall n|((nk))_N=p} x_2((n-j))_N - \sum_{\forall n|((nk))_N=p+M} x_2((n-j))_N\right]$

$Y'^{p}_{k} = \sum_{j=0}^{N-1} x_1(j) Y_{2_k}^{p-((jk))_N}$, using circular shift property

Let $q = ((jk))_N$, the terms $x_1(j)$ will have common multiplicand $Y_{2_k}^{p-q}$ if their index j is such that $q = ((jk))_N$ and $Y_{2_k}^{q+N/2} = -Y_{2_k}^{q}$

$Y'^{p}_{k} = \sum_{j=0}^{N-1} x_1(j) Y_{2_k}^{p-q}$

$Y'^{p}_{k} = \sum_{q=0}^{N-1} \sum_{((jk))_N=q} x_1(j) Y_{2_k}^{p-q} = \sum_{q=0}^{M-1} \sum_{((jk))_N=q} x_1(j) Y_{2_k}^{p-q} + \sum_{q=M}^{N-1} \sum_{((jk))_N=q} x_1(j) Y_{2_k}^{p-q}$

$Y'^{p}_{k} = \sum_{q=0}^{M-1} \sum_{((jk))_N=q} x_1(j) Y_{2_k}^{p-q} - \sum_{q=0}^{M-1} \sum_{((jk))_N=q+M} x_1(j) Y_{2_k}^{p-q}$

$Y'^{p}_{k} = \sum_{q=0}^{M-1} Y_{1_k}^{q} Y_{2_k}^{p-q} = \sum_{j=0}^{M-1} sY_{1_k}^{((jk))_N} Y_{2_k}^{\left((p-((jk))_N)\right)_M}$

When $p-q<0$, $Y_{2_k}^{(p-q)} = -Y_{2_k}^{((p-q))_M}$

$Y'^{p}_{k} = \sum_{j=0}^{M-1} sY_{1_k}^{((jk))_N} Y_{2_k}^{\left((p-((jk))_N)\right)_M}$, $s = \begin{cases} 1, ((jk))_N < p+1 \\ -1, ((jk))_N \geq p+1 \end{cases}$

Convolution in time domain changes to multiplication in frequency domain in the case of DFT while in MRT it remains as convolution itself among different phase terms corresponding to a given frequency.

2) Redundancy

1-D MRT maps an N- point sequence into MN coefficients where a number of coefficients have the same magnitude but different frequency and phase indices. Hence, it is highly redundant with two types of redundancies - complete redundancy and derived redundancy. Complete redundancy occurs when two coefficients have same magnitude but derived redundancy occurs when one coefficient can be obtained from a combination of other coefficients.

Detailed discussions on complete and derived redundancies are given in [7].

III. FORWARD 1-D GMRT

In [7], unique coefficients retained are arranged in increasing order of their GCD values between k & N after removal of complete and derived redundant coefficients from the MRT representation. Placement of 1-D GMRT in terms of divisors of N for $N = 12$ is as in Fig 2. All divisor frequencies that share same GCD value with respect to N forms a GCD packet represented by dark borders as in the figure. The coefficient Y_0^0 is computed and placed at location G(0). Subsequently unique MRT coefficients Y_1^p are computed and placed at locations G(1),G(2),G(3)…G($\Phi\left(\frac{N}{1}\right)+1$), where Φ is the Euler Totient Function [9]. Similarly, other GCD packets are sequentially placed in successive locations with increasing order of GCD values. The coefficients in a GCD packet are placed in increasing order of phase values, limited by $\Phi\left(\frac{N}{k}\right)$.

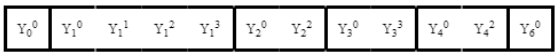

Fig. 2. Placement of 1-D GMRT [8] for $N = 12$

GMRT coefficients can be computed either by direct approach using (4) or by M-spacing based approach utilizing visual patterns of the coefficients using algorithms given in [7]. M-spacing based approach requires less computation time compared to direct approach as the size of the signal increases.

IV. RECONSTRUCTION OF ORIGINAL SIGNAL

Once a signal is transformed to any domain for any transform, reconstruction of original signal should be possible after processing the signal in the new domain. Reconstruction of original signal from 1-D GMRT requires identification of the coefficients with the required data element $x(n)$ involved in the computation.

The number of data elements involved in computation of coefficient Y_k^p, from (4), for a given value of k & p is governed by the linear congruence equations

$((nk))_N = p$ (5)

$((nk))_N = p + M$ (6)

where (5) & (6) give data elements to be added and subtracted respectively. If the linear congruence equation (5) is soluble then, as per number theoretic principles [9], it gives $g(k,N)$ solutions mod N. Its general solution can be written as $n = n_0 + t(N/g(k,N))$, where $0 \le t < g(k,N)$ and n_0 is the particular solution. Hence the distance between the data elements to be added to compute a given coefficient Y_k^p is $N/g(k,N)$. The same principle is applicable for (6) to find the data elements to be subtracted. The particular solution of (5) can be obtained as $n_0 = p/k$, and that of (6) is $n_0 = (p+M)/k$. Thus, the distance between data element to be added and the corresponding data element to be subtracted in a given coefficient is M/k. So, if the data element $x'(n)$ occurs with negative sign along with $x(n)$ in the coefficient Y_k^p then $n' = n + q\frac{M}{k} = n + q\frac{N}{2k}$. $x'(n)$ occur with same sign as that of $x(n)$ for frequency $k' = 2k$, $n' = n + q\frac{N}{k'}$. Thus, any element $x'(n)$ that occurs in reversed/same sign along with $x(n)$ in the MRT coefficient of frequency k, also occurs in same/reversed sign along with $x(n)$ in the MRT coefficient of frequency $k' = 2k$. This property is satisfied by power of 2 divisor frequencies only, hence the reconstruction formula has to involve MRT coefficients with power of 2 frequencies only.

In the computation of DFT coefficients, any frequency component depends on every data. In MRT, different frequencies are divided into variable number of phase terms and each phase term has variable number of data involvement. The total number of data involved in a particular frequency is always N, whatever be the number of phase terms. Thus a scaling by $\frac{1}{N}$ is involved in the inverse MRT computation or each unique MRT coefficient must be scaled by inverse of number of data points involved in the computation of that coefficient.

The number of data points (n_d) involved in the computation of a coefficient depends on total number of phase terms (n_p) associated with its frequency by the relation $n_d = \frac{N}{n_p}$ and

$$n_p = \begin{cases} \frac{M}{k} & , \ if\ k|M \\ \frac{N}{k} & , \ if\ k \nmid M \end{cases} \text{ then } n_d = \begin{cases} 2k & , \ if\ k|M \\ k & , \ if\ k \nmid M \end{cases}$$

If $k = 2^u$, then all coefficients are scaled by $\frac{1}{2^{u+1}}$ except for coefficient corresponding to highest power of 2 divisor frequency since it does not divide M. The phase indices of unique coefficients, in which $x(n)$ are present, can be found by multiplying n with each unique frequency k.

Hence reconstruction formula is

$$x(n) = \frac{1}{v} Y_{((v))_N}^{((n\,v))_N} + \sum_{u=0}^{\log_2 v - 1} \frac{1}{2^{u+1}} Y_{2^u}^{((2^u n))_N} \quad (7)$$

where v is the highest power of 2 divisor of N.

Equation (7) shows that power of 2 divisor frequencies with all phase terms are sufficient for signal reconstruction rather than all the divisor frequencies. But certain phase terms of power of 2 divisor frequencies were eliminated in the development of forward 1-D GMRT representation presented in [7] and considered all the divisor frequencies for the reconstruction of the original signal which involves estimation process to reconstruct eliminated coefficients. Thus the forward 1-D GMRT representation in [7] is modified in terms of power of 2 divisor frequencies and presented in the following section.

V. NEW FORWARD 1-D GMRT

The modified forward 1-D GMRT representation with all the phase components corresponding to power of 2 divisor frequencies is discussed below. The placement of coefficients corresponding to 1-D GMRT in terms of power of 2 divisor frequencies for $N = 12$ can be modified as in Fig 3.

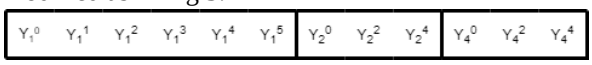

Fig. 3. Modified forward 1-D GMRT representation of $N = 12$

Size of each GCD packet in this type of placement is given by $\frac{M}{g}$ if $g|M$, where $g = \gcd(k, N)$ else it is $\frac{N}{g}$. Algorithm for forward and inverse 1-D GMRT is discussed below.

A. Algorithm for forward 1-D GMRT (M-spacing based approach)

1. Initialization

Input signal, $x(n)$, $0 \le n \le N-1$, $M = \frac{N}{2}$, $K = div(N)$, $A = 0$, $B = 0$,

GMRT array G= 0, v = power of highest power of 2 divisor of N

2. To compute A and B

For $i = 0: M-1$

$A(i) = x(i) + x(i+M)$

$B(i) = x(i) - x(i+M)$

End

3. To compute power of 2 divisors of N

For $i = 0: v$

$d(i) = 2^i$

End

4. To compute coefficients corresponding to $k = 1$

c =1

For $i = 0: M-1$

$G(c) = B(i)$

$c = c + 1$

End

5. To compute other coefficients

For $i = 1: v$

$k = d(i); k1 = k/2;$

$Nbyk = N/k$

If $k|M$

$np = M/k$

Else

$np = N/k$

Endif

For $j = 0: np-1$

If $k|M$

$p = j.k$

Else

$p = j.k1$

Endif

For $w = 0: k-1$

$n_1 = \frac{p}{k} + w.Nbyk$

$n_2 = \frac{p+M}{k} + w.Nbyk$

If (n_1 is integer) && ($n_1 < M$)

$G(c) = G(c) + A(n_1)$

Endif

If (n_2 is integer) && ($n_2 < M$)

$G(c) = G(c) - A(n_1)$

Endif

End %end of w loop

c=c+1

End % end of j loop

End % end of i loop

If $mod(\log_2 N) = 0$ % applicable when N is a power of 2

Circshift(G, 1)

Endif

B. Algorithm for inverse 1-D GMRT

1. Initialization

GMRT array G of size N, $M = N/2$

2. Computation of power of 2 divisors

If N is a power of 2 $v = \log_2 N - 1$

Else v = power of highest power of 2 divisor of N

For $i = 0: v$

$d(i) = 2^i$

End

3. If N is a power of 2 %Contribution of $G(0)$,

%applicable only when N is a power of 2
For $n = 0: N-1$
$x(n) = \frac{G(0)}{N}$
End
Endif
4. Contributions of other coefficients
For $n = 0: N-1$
If N is a power of 2
$a = 1$
Else $a = 0$
Endif
For $i = 0: v$
$k = d(i), z = \left((nk)\right)_N$,$k1 = k/2$
$Mbyk = M/k, Nbyk = N/k$
If $k|M$
$n_d = N/Mbyk$
$u = Mbyk$
Else
$n_d = N/Nbyk$
$u = Nbyk$
Endif
For $j = 0: u-1$
If $k|M$
$p = j.k$
Else
$p = j.k1$
Endif
If $z == p$
$x(n) = x(n) + \frac{1}{n_d} G(a)$
Else if $z == p + M$
$x(n) = x(n) - \frac{1}{n_d} G(a)$
Endif
$a = a + 1$
End % end of j loop
End % end of i loop
End % end of n loop

VI. PROPERTIES OF 1-D GMRT

1) 1-D GMRT basis array

Any data can be expressed as linear combination of basis array. Visual representation of MRT coefficients [4] can be used to obtain basis array of 1-D GMRT which is shown in Fig.4 for $N = 12$. It has values +1, -1 or 0 and hence 1-D GMRT form an integer-to-integer transform with integer arithmetic.

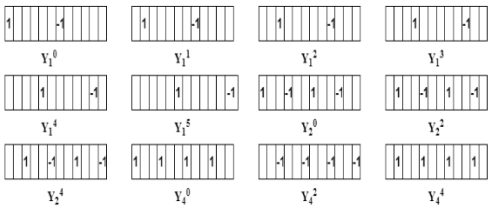

Fig. 4. Basis array of 1-D GMRT for $N = 12$

Basis array of GMRT representation can be expressed as in (10) and (11). The key parameters involved in the computation of basis array for GMRT are index g of the GCD packet given by $g = gcd(k, N)$, and the index i of the coefficient within the GCD packet.

$$A_{g,i}(n) = \begin{cases} 1, \ if \ \left((ng)\right)_N - g.i = 0 \\ -1, \ if \ \left((ng)\right)_N - g.i = M \\ 0, \ otherwise \end{cases}, \quad if \ g|M$$

(10)

$$A_{g,i}(n) = \begin{cases} 1, \ if \ \left((ng)\right)_N - \frac{g.i}{2} = 0 \\ -1, \ if \ \left((ng)\right)_N - \frac{g.i}{2} = M \\ 0, \ otherwise \end{cases}, \quad if \ g \nmid M$$

(11)

GMRT can be represented in terms of basis array as

$G_g(i) = \langle X, A_{g,i} \rangle = \sum_{n=0}^{N-1} x(n) \, A_{g,i}(n)$
(12)

$A_{g,i}$ is the basis array corresponding to i th element of g^{th} GCD packet.

2) Linearity

If $x_1(n) \overset{GMRT}{\longleftrightarrow} G_{1_g}(j)$ and $x_2(n) \overset{GMRT}{\longleftrightarrow} G_{2_g}(j)$ then, $a_1 x_1(n) + a_2 x_2(n) \overset{MRT}{\longleftrightarrow} a_1 G_{1_g}(j) + a_2 G_{2_g}(j)$ for any real valued constants a_1 and a_2

Proof
From (10), (11) & (12) $\sum_{\forall n|((ng))_N = gj} x(n) - \sum_{\forall n|((ng))_N = gj+M} x(n) = G_g(j)$ then
$\because \sum_{\forall n|((ng))_N = gj} \left(a_1 x_1(n) + a_2 x_2(n)\right) - \sum_{\forall n|((ng))_N = gj+M} \left(a_1 x_1(n) + a_2 x_2(n)\right)$
$= \sum_{\forall n|((ng))_N = gj} a_1 x_1(n) - \sum_{\forall n|((ng))_N = gj+M} a_1 x_1(n) + \sum_{\forall n|((ng))_N = gj} a_2 x_2(n) - \sum_{\forall n|((ng))_N = gj+M} a_2 x_2(n)$
$= a_1 \left(\sum_{\forall n|((ng))_N = gj} x_1(n) - \sum_{\forall n|((ng))_N = gj+M} x_1(n)\right) + a_2 \left(\sum_{\forall n|((ng))_N = gj} x_2(n) - \sum_{\forall n|((ng))_N = gj+M} x_2(n)\right)$
$= a_1 G_{1_g}(j) + a_2 G_{2_g}(j)$

3) Orthogonality

GMRT basis arrays are orthogonal to each other confirming the relationship

$$\langle A_{g,j}(n), A_{g',j'}(n)\rangle = \begin{cases} c, & g = g' and\ j = j' \\ 0, & otherwise \end{cases}$$

4) Redundancy factor ($R_g(j)$)

Redundancy present in MRT is eliminated in GMRT representation by retaining only unique coefficients. The number of redundant elements associated with each coefficient in the GMRT representation is expressed by the redundancy factor $R_g(j)$. It is given by $\frac{M}{g}$ if $g|M$ otherwise $\frac{N}{g}$. In other words, redundancy factor of a given GMRT coefficient is determined by the size n_d of the GCD packet to which it belongs. Fig. 5 shows redundancy factor for GMRT representation when $N = 12$.

Fig. 5. Redundancy factor of GMRT for $N = 12$

5) Parseval's theorem

Energy is to be conserved whenever a signal is transformed from one domain to another, which can be verified using Parseval's theorem. Since many redundant coefficients are removed in the GMRT representation, it is important to consider the redundancy factor while analyzing its energy conservation property. Parseval's theorem for GMRT representation is given by

$$\sum_{n=0}^{N-1} x^2(n) = \begin{cases} \frac{1}{N}\sum_{\forall g}\sum_{j=0}^{\frac{M}{g}-1} R_g(j)\left|G_g(j)\right|^2, & if\ g|M \\ \frac{1}{N}\sum_{\forall g}\sum_{j=0}^{\frac{N}{g}-1} R_g(j)\left|G_g(j)\right|^2, & if\ g \nmid M \end{cases} \quad (13)$$

Proof

$$\frac{1}{N}\sum_{\forall g}\sum_{j=0}^{\frac{M}{g}-1} R_g(j)\left|G_g(j)\right|^2 = \frac{1}{N}\sum_{\forall g}\sum_{j=0}^{\frac{M}{g}-1} R_g(j)\left|\sum_{w=0}^{g-1} x_{\frac{gj+wN}{g}} - x_{\frac{gj+(2w+1)M}{g}}\right|^2 = \sum_{n=0}^{N-1} x^2(n)$$

$$\frac{1}{N}\sum_{\forall g}\sum_{j=0}^{\frac{N}{g}-1} R_g(j)\left|G_g(j)\right|^2 = \frac{1}{N}\sum_{\forall g}\sum_{j=0}^{\frac{N}{g}-1} R_g(j)\left|\sum_{w=0}^{g-1} x_{\frac{(gj)/2+wN}{g}} - x_{\frac{(gj)/2+(2w+1)M}{g}}\right|^2 = \sum_{n=0}^{N-1} x^2(n)$$

6) Signal reversal

If $x(n) \overset{GMRT}{\longleftrightarrow} G_g(j)$ and $x((-n))_N \overset{GMRT}{\longleftrightarrow} Z_g(j)$,

then $Z_g(j) = \begin{cases} -G_g(M-gj), j \neq 0, g|M \\ -G_g\left(M-\frac{gj}{2}\right), j \neq 0, g \nmid M \\ G_g(j), j = 0 \end{cases}$

Proof

$Z_g(j) = \sum_{\forall n|((ng))_N = gj} x((-n))_N - \sum_{\forall n|((ng))_N = gj+M} x((-n))_N$

Let $((-n))_N = \left((N-n)\right)_N = n'$

$Z_g(j) = \sum_{\forall n'|((((-n'))_N\, g))_N = gj} x(n') - \sum_{\forall n'|((((-n'))_N\, g))_N = gj+M} x(n')$

$Z_g(j) = \sum_{\forall n'|((n'g))_N = ((N-gj))_N} x(n') - \sum_{\forall n'|((n'g))_N = \left((N-(gj+M))\right)_N} x(n')$

$Z_g(j) = \sum_{\forall n'|((n'g))_N = ((M-gj+M))_N} x(n') - \sum_{\forall n'|((n'g))_N = ((M-gj))_N} x(n')$

$Z_g(j) = -G_g(M-gj)$

$$\therefore Z_g(j) = \begin{cases} -G_g(M-gj), j \neq 0, g|M \\ -G_g\left(M-\frac{gj}{2}\right), j \neq 0, g \nmid M \\ G_g(j), j = 0 \end{cases}$$

VII. ALGORITHM TO DERIVE ALL FREQUENCIES FROM 1-D GMRT REPRESENTATION

The forward 1-D GMRT representation has coefficients corresponding to power of 2 divisor frequencies only. But many applications require coefficients corresponding to all frequencies. In such cases, coefficients corresponding to other frequencies can be derived using the following algorithm.

1. Initialization

Let the packets of all frequencies be U_decomp = [], G be the 1-D GMRT, G_decomp be the packets of 1-D GMRT, $K = div(N)$, $s = size(K)$, v = power of highest power of 2 divisor of N, o =odd divisors of N, $so = size(o)$

2. To compute power of 2 divisors of N

For $i = 0{:}\, v$

$$d(i) = 2^i$$

End

%Decomposing 1-D GMRT packets

$npac = v + 1$ % number of packets

For $i = 0{:}\, v$

$k = d(i)$

If $k|M$

$Psz(i) = M/k$ %packet size

Else

$Psz(i) = N/k$
Endif
End %end for loop
G_decomp= zeros($npac$, Psz (0))
$Pst = 1$ % start of packet
For $i = 0: npac - 1$
$Pend = Pst + Psz(i) - 1$
G_decomp $(i, 1: Psz(i))$= G $(Pst: Pend)$
$Pst = Pend + 1$
End %end for loop

3. Placement of packets of 1-D GMRT into corresponding locations of U_decomp

For $i = 0: v$
U_decomp$(d(i), :) = G$_decomp$(i, :)$
End

4. Compute packet size of non-power of 2 divisor frequency

For $i = 0: s - 1$
$temp = K(i)$
If $temp|M$
$Psz(i) = M/temp$
Else
$Psz(i) = N/temp$
Endif
End

5. Compute the coefficients of non-power of 2 divisor frequencies using derived redundancy relation

For $i = 0: v$
$K1 = d(i)$ %power of 2 divisor frequency
$K1\_ar = G\_decomp(i, :)$
For $a = 0: so - 1$
$K2 = K1.o(a)$ %non power of 2 divisor frequency
$K2\_in = find(K == K2)$ %index of $K2$ in K
$K2\_ar = []$
For $i_1 = 0: Psz(K2\_in) - 1$
If $K2|M$
$p2 = K2.i_1$; $p = p2/K2$
$Mbyo = M/K2$;
$pend = p + (o(a) - 1).Mbyo$
Else
$p2 = (K2.i_1)/2$; $p = 2.(p2/K2)$
$Mbyo = 2.(M/K2)$;
$pend = p + (o(a) - 1).Mbyo$
Endif
$K2\_end = 0$; $count = 0$
For $j = p: Mbyo: pend$
$K2\_end = K2\_end + (-1^{count}).K1\_ar(j)$
$count = count + 1$
End %end of j
$K2\_ar = [K2\_ar, K2\_end]$
End % end of i_1
U_decomp$\big(K2_in, 1: Psz(K2_in)\big) = K2_ar$
End % end of a
End %end of i

6. Find integers between 1 to $N - 1$ coprime to N

$phyofN = 1$
$k\_coprtoN(phyofN) = 1$
For $i1 = 2: N - 1$
If $gcd(i1, N) == 1$
$phyofN = phyofN + 1$
$k\_coprtoN(phyofN) = i1$
Endif
End

7. Compute the coefficients of non-divisor frequencies using redundancy relations

For $i = 0: s - 3$
$k1 = K(i)$
For $i1 = 2: phyofN$
$frek1 = \big((k\_coprtoN(i1) * k1)\big)_N$
$k1\_in = find(K == k1)$
For $j = 0: Psz(k1\_in) - 1$
If $k1|M$
$pk1 = k1.j$ %phase of $k1$
Else
$pk1 = (k1.j)/2$
Endif
$kpn = \big((k\_coprtoN(i1).pk1)\big)_N$
$kpm = \big((k\_coprtoN(i1).pk1)\big)_M$
$g = gcd(frek1, N)$
If $g|M$
$jfrek1 = (kpm/g)$
Else
$jfrek1 = (2.kpm/g)$
Endif
If $kpn < M$

U_decomp$(frek1, jfrek1)$ =U_decomp$(k1, j)$
Else
U_decomp$(frek1, jfrek1)$ = $-$U_decomp$(k1, j)$
Endif
End %end of j
End % end of $i1$
End % end of i

VIII. APPLICATION

GMRT is a general purpose signal processing tool that can be applied for a wide range of applications. Its application in a direct speech to speech machine

translation system from Sanskrit to Malayalam language is explored in this paper. Sanskrit corpora are obtained from the Digital Corpus of Sanskrit (DCS) (http://kjc-fs-cluster.kjc.uni-heidelberg.de/dcs /index.php), developed by Oliver Hellwig [10] and Computational linguistics R&D at JNU-India (http://sanskrit.jnu.ac.in/sbg/index.jsp) [11], MTIL, dataset, TDIL dataset, Open subtitles, and other sources. They are pre-processed to make different sentences, with a maximum of 10 words in a sentence. The dataset thus constructed contains 2,54,700 Sanskrit sentences. Corresponding Malayalam sentences are manually constructed by consulting linguistic experts in both Sanskrit and Malayalam languages. Further, these sentences are recorded using the Recorder app on Android phones and the Audacity platform as speech with the help of 150 volunteers who are proficient in both Sanskrit and Malayalam languages. The maximum duration of a sentence in the speech database is 3 seconds with 750,000 samples and zero padding is used for smaller sentences. So, the database contains more than 200 hours of Sanskrit and Malayalam data.

Modern speech translation systems employ a three-step methodology in which the input speech signal is first translated into appropriate text using speech recognition technology, followed by a text-to-text translation stage and finally the translated speech is synthesized from the translated text. Hence Direct speech to speech [DSS] translation without the use of text translations is used since these systems are susceptible to different errors in speech recognition. Neural Machine Translation (NMT) is an end-to-end deep learning model for automated translation with high translation quality. Generally, NMT models incorporate an Encoder and Decoder, which are implemented using LSTM and trained mutually [12]. The encoder that encodes the meaning of the sentence produces a context vector from the input source sentence, which is further processed by the decoder to produce translation.

A Vanilla NMT model [13], designed by varying the number of hidden layers and the number of neurons in each layer with SoftMax as the activation function, is employed for translation. The model is initially trained using a single hidden layer and then trained with two hidden layers by varying the number of neurons used for both the encoders and decoders from 1 to 500. The Adam optimizer is used as the optimization algorithm with a learning rate of 0.001 [13]. Beam search with a beam size of 5 is used by the decoder during the translation phase. The speech signal is windowed for short-time processing to account for its non-stationary nature. Feature vectors are extracted using the wavelet transform (WT), SMRT or GMRT, and their performance is evaluated. The extracted feature vectors are given as input to the vanilla NMT model, whose output is converted back to speech using inverse WT/SMRT/GMRT respectively. A basic block diagram of the Sanskrit-Malayalam direct speech to speech machine translation system is shown in Fig. 6.

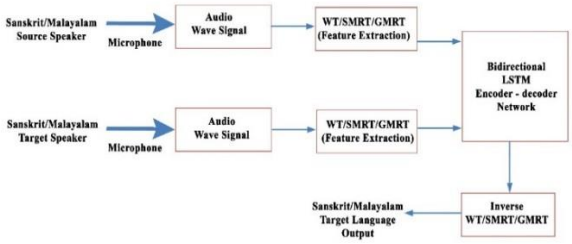

Fig. 6. Direct Speech to Speech Translation

Short-time (ST) feature extraction with a frame size of 256 samples is implemented using Daubechies 4-tap, 6-tap, 8-tap and 10-tap wavelets, Harr wavelet and Wavelet Packet Decomposition (WPD). Manual translation scores (S_1, S_2) [13] are determined in each case and a sample set of results with training time in hours (T) is displayed in Tables I and II. The test results demonstrated that adopting Daubechies 4-tap wavelet feature extraction, the encoder-decoder model with 425 neurons in the first hidden layer and 430 neurons in the second hidden layer, generates a translation score of 61.1% and that using Daubechies 6-tap wavelet produces a translation score of 62.9% with 420 and 435 neurons respectively, in the first and second hidden layers. Similarly, Daubechies 8-tap and 10-tap wavelets produced translation scores of 61.3% and 61.2% with (425, 430) and (430, 435) neuron combinations in the two layers, respectively.

TABLE I
SANSKRIT TO MALAYALAM SPEECH MODEL USING ST DAUBECHIES 4-TAP,6-TAP AND 8-TAP WAVELET

H1			H2			S_1			S_2			T(h)		
4-tap	6-tap	8-tap	4-tap	6-tap	8-tap	4-tap	6-tap	8-tap	4-tap	6-tap	8-tap	4-tap	6-tap	8-tap
16	16	16	0	0	0	56.4	56.6	56.8	56.2	56.5	56.6	785	787	786
32	32	32	0	0	0	56.2	56.4	56.3	56.3	56.5	56.2	786	789	789
64	64	64	0	0	0	56.6	56.8	56.5	56.1	56.5	56.6	788	792	794
128	128	128	0	0	0	56.6	56.5	56.7	56.3	56.2	56.5	795	794	796
256	256	256	0	0	0	56.8	56.9	56.8	56.4	56.3	56.6	797	798	799
300	300	300	0	0	0	56.5	56.9	56.7	56.4	56.5	56.3	798	796	798
350	350	350	0	0	0	57.5	57.4	57.3	56.9	56.8	56.9	812	815	817
400	400	400	0	0	0	57.1	57.7	57.2	56.8	56.9	56.8	815	818	819
425	450	450	0	0	0	57.3	57.7	57.5	57.4	57.6	57.9	823	826	824
450	470	470	0	0	0	57.2	57.6	57.3	57.3	57.5	57.7	825	827	828
500	500	500	0	0	0	57.2	57.7	57.2	57.1	57.5	57.3	827	829	832
16	16	16	16	16	16	58.3	58.6	58.4	58.2	58.5	58.3	853	857	862
32	32	32	32	32	32	58.4	58.5	58.2	58.3	58.6	58.3	854	856	863
64	64	64	64	64	64	58.9	59.1	58.4	58.8	58.9	58.2	858	861	867
128	128	128	128	128	128	59.2	59.3	59.3	59.3	59.1	59.1	859	864	864
256	256	256	256	256	256	59.4	59.6	59.2	59.5	59.7	59.3	863	868	871
300	300	300	300	300	300	60.1	60.6	60.1	59.9	60.8	60.4	864	871	873
350	350	350	350	350	350	60.2	60.9	60.5	60.3	61.1	60.6	866	874	878
400	400	400	400	400	400	60.4	61.4	60.6	60.5	61.5	60.5	868	878	881
425	**420**	**425**	**430**	**435**	**430**	**61.1**	**62.8**	**61.3**	**60.9**	**62.9**	**61.5**	**872**	**883**	**885**
450	450	450	450	450	450	60.6	62.1	61.1	60.5	62.2	61.3	876	886	889
500	500	500	500	500	500	60.2	61.6	60.8	60.1	61.7	60.9	879	889	893

TABLE II
SANSKRIT TO MALAYALAM SPEECH MODEL USING ST DAUBECHIES 10-TAP, WPD & HARR WAVELETS

H1			H2			S_1			S_2			T(h)		
10-tap	WPD	Harr	10-tap	WPD	Harr	10-tap	WPD	Harr	10-tap	WPD	Harr	10-tap	WPD	Harr
16	16	16	0	0	0	56.2	56.5	56.1	56.5	56.7	56.3	788	813	784
32	32	32	0	0	0	56.1	56.2	56.3	56.1	56.5	56.4	789	817	786
64	64	64	0	0	0	56.3	56.7	56.5	56.2	56.8	56.3	797	825	787
128	128	128	0	0	0	56.4	56.3	56.3	56.2	56.1	56.1	798	828	792
256	256	256	0	0	0	56.5	56.6	56.5	56.4	56.8	56.3	810	846	795
300	300	300	0	0	0	56.5	57.1	56.8	56.2	56.8	56.7	812	852	798
350	350	350	0	0	0	57.2	57.5	57.1	56.5	57.6	56.8	816	867	810
400	400	400	0	0	0	57.1	57.8	57.3	56.8	57.9	56.9	823	885	814
450	450	425	0	0	0	57.2	57.6	57.1	57.4	57.4	57.1	828	898	817
475	470	450	0	0	0	57.2	57.7	57.1	57.3	57.5	57.4	830	905	821
500	500	500	0	0	0	57.1	57.9	57.3	57.2	57.8	57.2	835	913	828
16	16	16	16	16	16	58.2	58.2	58.2	58.1	58.1	58.3	865	923	835
32	32	32	32	32	32	58.1	58.4	58.5	58.2	58.2	58.4	866	938	836
64	64	64	64	64	64	58.2	58.7	58.8	58.1	58.8	58.7	868	941	838
128	128	128	128	128	128	59.3	58.8	58.9	59.1	58.9	58.7	864	945	841
256	256	256	256	256	256	59.1	58.9	59.1	59.2	59.1	59.2	875	948	844
300	300	300	300	300	300	59.7	59.8	60.2	60.1	59.6	60.3	878	953	845
350	350	350	350	350	350	60.2	60.1	60.4	60.1	60.2	60.5	882	958	848
400	400	400	400	400	400	60.2	60.3	60.6	60.1	60.4	60.8	887	962	849
430	**435**	**425**	**435**	**440**	**425**	**61.1**	**60.6**	**61.3**	**61.2**	**60.8**	**61.5**	**889**	**967**	**852**
450	450	450	450	450	450	60.9	60.1	60.9	60.8	60.4	61	893	972	858
500	500	500	500	500	500	60.1	59.7	60.3	60.2	59.4	60.4	897	976	859

Here, wavelet packet analysis is carried out using the Harr wavelet for 9 decomposition levels since the frame size is 256 samples and SMRT will have 9 packets. At each level, 4 features are obtained by averaging the wavelet-packet coefficients of the LL, LH, HL, and HH bands. Thus, a total of 36 features are obtained from the wavelet packet for each frame. A translation score of 60.8% is obtained for the encoder-decoder model with 435 and 440 neurons in the first and second hidden layers using WPD and the model with two hidden layers of 425 neurons each employing the Harr wavelet feature extraction method generates a translation score of 61.5%.

Prior to the implementation of a speech translation system using GMRT, it is necessary to find out the best frame size for analysis. Since speech is a quasi-stationary signal, its local characteristics must be analyzed to extract relevant information. The frame sizes for GMRT can be any even integer value, unlike SMRT, with frame sizes of power of 2, makes it easier to analyze signals locally. Table III and IV show the performance of the NMT system implemented by varying the frame size of the signal and the number of first and second hidden layer neurons, respectively. Table III shows that the frame size of the signal is varied from 130 to 512 and the results indicate that the score steadily improved from 43.2% to 72.1% as the frame size was increased from 130 to 248; on further increases, the score steadily dropped down to 51.2% for the frame size of 300. Table IV reveals that the NMT model with 410 and 415 hidden neurons, respectively, produces a translation score of 72.1% with a training period of 992 hours. The frame size of 256 selected for SMRT produced a score of 62.5%. So an improvement of 10% is achieved from a GMRT based NMT system with a reduced frame size as compared to SMRT.

TABLE III
PERFORMANCE COMPARISON OF GMRT BASED SYSTEM FOR DIFFERENT FRAME SIZES

Frame Size	Manual Score	Frame Size	Manual Score	Frame Size	Manual Score	Frame Size	Manual Score
130	43.2	176	52.4	222	61.7	268	62.13
132	43.6	178	52.5	224	61.8	270	61.06
134	44.1	180	53.2	226	62.4	272	60.3
136	44.4	182	53.6	228	62.7	274	59.2
138	44.8	184	54.1	230	63.3	276	58.6
140	45.5	186	54.6	232	63.6	278	58.3
142	45.6	188	54.7	234	64.3	280	57.4
144	46.3	190	55.3	236	64.4	282	57.1
146	46.4	192	55.6	238	64.8	284	56.5
148	46.8	194	56	240	65.3	286	56.1
150	47.2	196	56.4	242	65.4	288	55.2
152	47.6	198	56.7	244	65.9	290	54.3
154	48.2	200	57.2	246	68.4	292	53.8
156	48.4	202	57.6	248	72.1	294	52.6
158	48.9	204	57.8	250	70.62	296	52.1
160	49.2	206	58.4	252	68.41	298	51.5
162	49.6	208	58.8	254	65.37	300	51.2
164	50.3	210	59.3	256	62.5		
166	50.4	212	59.8	258	62.48		
168	50.7	214	59.9	260	62.44		
170	51.2	216	60.2	262	62.32		
172	51.6	218	60.9	264	62.27		
174	52.2	220	61.3	266	62.2		

TABLE IV
SANSKRIT TO MALAYALAM SPEECH MODEL USING SMRT & GMRT

H1		H2		S_1		S_2		T(h)	
SMRT	GMRT	SMRT	GMRT	SMRT	GMRT	SMRT	GMRT	SMRT	GMRT
16	16	0	0	56.5	57.8	56.7	57.6	768	796
32	32	0	0	56.2	58.1	56.5	58.3	773	810
64	64	0	0	56.7	58.8	56.8	58.9	787	817
128	128	0	0	56.3	59.6	56.1	59.5	790	825
256	256	0	0	56.6	60.8	56.8	60.7	793	832
300	300	0	0	57.1	61.5	56.8	61.6	794	840
350	350	0	0	57.5	62.8	57.6	62.9	810	856
400	400	0	0	57.8	64.2	57.9	64.3	812	868
450	450	0	0	57.6	65.8	57.4	65.9	815	883
470	470	0	0	57.7	66.3	57.5	66.7	817	885
500	500	0	0	57.9	67.2	57.8	67.3	822	892
16	16	16	16	58.4	68.4	59.3	68.5	833	915
32	32	32	32	58.3	69.5	59.8	69.6	837	921
64	64	64	64	58.8	69.7	59.4	69.8	845	934
128	128	128	128	59.1	69.9	58.9	69.9	847	942
256	256	256	256	59.4	70.2	59.5	70.1	849	947
300	300	300	300	60.4	70.4	60.2	70.5	851	956
350	350	350	350	60.6	70.8	60.5	70.7	852	968
400	400	400	400	61.1	71.3	61.3	71.5	854	974
420	**410**	**430**	**415**	**62.4**	**72.1**	**62.5**	**71.9**	**856**	**992**
450	450	450	450	62.1	69.3	62.2	69.4	859	994
500	500	500	500	61.7	68.7	61.8	68.8	862	998

Hence, GMRT offers better performance in comparison to wavelet and SMRT based NMT systems for translation from Sanskrit to Malayalam

IX. CONCLUSION

A new transform representation, 1-D GMRT, suitable for 1-D signals of any length is derived from unique MRT coefficients. It is an integer-to-integer transform and computations require only real additions. General properties, visual representation and basis function along with its application in speech translation system are outlined. This is a general purpose tool suitable for signal processing applications.

IX. DECLARATION

Ethical approval

Not applicable

Competing interest

Authors have no competing interests as defined by Springer, or other interests that might be perceived to influence the results and/or discussion reported in this paper.

Author's contribution

Development of transform: L.S.Panicker

Development of application: Rahul. C/ L.S. Panicker

Research Supervision: Dr. Gopikakumari. R

Funding

Not applicable

Availability of data

Access link is provided within the article

REFERENCES

[1] R. Gopikakumari, "Investigations on the development of an ANN model and visual manipulation approach for 2D DFT computation in image processing," PhD Thesis, Cochin University of Science and Technology, Kochi, India, 1998. [Online]. Available: http://dyuthi.cusat.ac.in/purl/3526

[2] R. C. Roy, "Development of a New Transform : Mrt," PhD Thesis, Cochin University of Science and Technology, Kochi, India, 2009. [Online]. Available: http://dyuthi.cusat.ac.in/purl/2688

[3] R. C. Roy and R. Gopikakumari, "A new transform for 2-D signal representation (MRT) and some of its properties," in 2004 International Conference on Signal Processing and Communications, SPCOM, 2004, no. 2, pp. 363–367. doi: 10.1109/spcom.2004.1458423.

[4] V. Bhadran, "Development & Implementation of Visual Approach and Parallel Distributed Architecture for 2-D DFT & UMRT computation," PhD Thesis, Cochin University of Science and Technology, Kochi, India, 2009. [Online]. Available: http://dyuthi.cusat.ac.in/purl/5416

[5] V. L. Jaya and R. Gopikakumari, "Sequency-based mapped real transform: properties and applications," Signal, Image Video Process., vol. 11, no. 8, pp. 1551–1558, 2017, doi: 10.1007/s11760-017-1119-2.

[6] B. Manju, "Software Hardware Co-development for SMRT based Texture Analysis Applied in Medical and Non Medical Images," PhD Thesis, Cochin University of Science and Technology, Kochi, India, 2019. [Online]. Available: http://dyuthi.cusat.ac.in/purl/5481

[7] L. S. Panicker and R. Gopikakumari, "1-D GMRT : GCD based Mapped Real Transform for 1-D Signals," in *2022 3rd International Conference for Emerging Technology (INCET)*, 2022, pp. 1–5. doi: 10.1109/INCET54531.2022.9824169.

[8] A. Oppenheim and R. Schafer, *Discrete-Time Processing- Second Edition*, 2nd ed. Pearson Education, 1999. doi: 10.5555/294797.

[9] G.H. Hardy and E.M. Wright, *An Introduction to the Theory of Numbers, G.H. Hardy and E.M. Wright*, 6th ed., vol. 51, no. 3. 2008.

[10] O. Hellwig and S. Nehrdich, "Sanskrit word segmentation using character-level recurrent and convolutional neural networks," in *Proceedings of the 2018 Conference on Empirical Methods in Natural Language Processing, EMNLP 2018*, 2018, pp. 2754–2763. doi: 10.18653/v1/d18-1295.

[11] R. G. Rahul, C., "Multilingual Identification Using Deep Learning," *Intell. Sustain. Syst. Springer, Singapore*, pp. 589–598, 2022.

[12] M. Morishita, J. Suzuki, and M. Nagata, "NTT Neural Machine Translation Systems at WAT 2019," *IJCNLP 2019 - 6th Work. Asian Transl. WMT 2019 - Proc. Work.*, pp. 99–105, 2019.

[13] R. Chingamtotattil and R. Gopikakumari, "Neural machine translation for Sanskrit to Malayalam using morphology and evolutionary word sense disambiguation," *Indones. J. Electr. Eng. Comput. Sci.*, vol. 28, no. 3, pp. 1709–1719, 2022, doi: 10.11591/ijeecs.v28.i3.pp1709-1719.